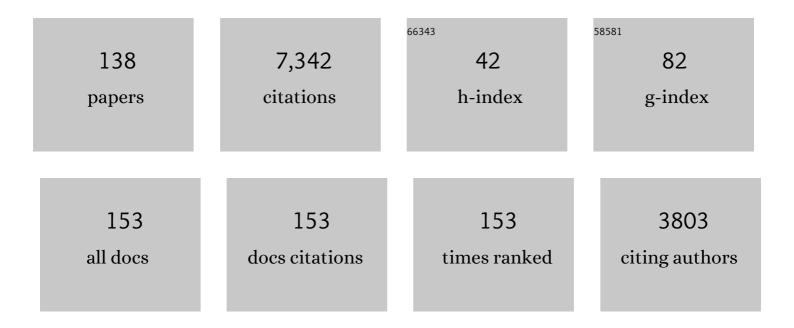
Javier Escartin

List of Publications by Year in descending order

Source: https://exaly.com/author-pdf/4031690/publications.pdf Version: 2024-02-01



#	Article	IF	CITATIONS
1	Corrugated slip surfaces formed at ridge–transform intersections on the Mid-Atlantic Ridge. Nature, 1997, 385, 329-332.	27.8	453
2	Central role of detachment faults in accretion of slow-spreading oceanic lithosphere. Nature, 2008, 455, 790-794.	27.8	407
3	Modes of seafloor generation at a melt-poor ultraslow-spreading ridge. Geology, 2006, 34, 605.	4.4	337
4	Oceanic core complexes and crustal accretion at slow-spreading ridges. Geology, 2007, 35, 623.	4.4	302
5	Strength of slightly serpentinized peridotites: Implications for the tectonics of oceanic lithosphere. Geology, 2001, 29, 1023.	4.4	280
6	Discovery of a magma chamber and faults beneath a Mid-Atlantic Ridge hydrothermal field. Nature, 2006, 442, 1029-1032.	27.8	248
7	Widespread active detachment faulting and core complex formation near 13° N on the Mid-Atlantic Ridge. Nature, 2006, 442, 440-443.	27.8	243
8	Constraints on deformation conditions and the origin of oceanic detachments: The Mid-Atlantic Ridge core complex at 15°45′N. Geochemistry, Geophysics, Geosystems, 2003, 4, .	2.5	234
9	Effects of serpentinization on the lithospheric strength and the style of normal faulting at slow-spreading ridges. Earth and Planetary Science Letters, 1997, 151, 181-189.	4.4	225
10	Oceanic detachment faults focus very large volumes of black smoker fluids. Geology, 2007, 35, 935.	4.4	205
11	Nondilatant brittle deformation of serpentinites: Implications for Mohr-Coulomb theory and the strength of faults. Journal of Geophysical Research, 1997, 102, 2897-2913.	3.3	203
12	Mid-Atlantic Ridge–Azores hotspot interactions: along-axis migration of a hotspot-derived event of enhanced magmatism 10 to 4 Ma ago. Earth and Planetary Science Letters, 1999, 173, 257-269.	4.4	190
13	Direct geological evidence for oceanic detachment faulting: The Mid-Atlantic Ridge, 15°45′N. Geology, 2002, 30, 879.	4.4	188
14	Dynamic control on serpentine crystallization in veins: Constraints on hydration processes in oceanic peridotites. Geochemistry, Geophysics, Geosystems, 2007, 8, n/a-n/a.	2.5	187
15	Fault rotation and core complex formation: Significant processes in seafloor formation at slowâ€spreading midâ€ocean ridges (Midâ€Atlantic Ridge, 13°–15°N). Geochemistry, Geophysics, Geosyste 2008, 9, .	2m 2, 5	186
16	Drilling constraints on lithospheric accretion and evolution at Atlantis Massif, Mid-Atlantic Ridge 30°N. Journal of Geophysical Research, 2011, 116, .	3.3	112
17	Relationships between the microstructural evolution and the rheology of talc at elevated pressures and temperatures. Earth and Planetary Science Letters, 2008, 268, 463-475.	4.4	105
18	Spatial and temporal distribution of seismicity along the northern Mid-Atlantic Ridge (15°-35°N). Journal of Geophysical Research, 2003, 108, .	3.3	99

#	Article	IF	CITATIONS
19	Seismic structure across the rift valley of the Mid-Atlantic Ridge at 23°20′ (MARK area): Implications for crustal accretion processes at slow spreading ridges. Journal of Geophysical Research, 2000, 105, 28411-28425.	3.3	98
20	Tectonic structure, evolution, and the nature of oceanic core complexes and their detachment fault zones (13°20′N and 13°30′N, Mid Atlantic Ridge). Geochemistry, Geophysics, Geosystems, 2017, 18, 14	51-1482.	94
21	Ultramafic exposures and the gravity signature of the lithosphere near the Fifteen-Twenty Fracture Zone (Mid-Atlantic Ridge, 14°–16.5A°N). Earth and Planetary Science Letters, 1999, 171, 411-424.	4.4	90
22	Crustal thickness of V-shaped ridges south of the Azores: Interaction of the Mid-Atlantic Ridge (36°-39°N) and the Azores hot spot. Journal of Geophysical Research, 2001, 106, 21719-21735.	3.3	90
23	Quantifying tectonic strain and magmatic accretion at a slow spreading ridge segment, Mid-Atlantic Ridge, 29ŰN. Journal of Geophysical Research, 1999, 104, 10421-10437.	3.3	83
24	Serpentinization and associated hydrogen and methane fluxes at slow spreading ridges. Geophysical Monograph Series, 2010, , 241-264.	0.1	83
25	Detachments in Oceanic Lithosphere: Deformation, Magmatism, Fluid Flow, and Ecosystems. Eos, 2011, 92, 31-31.	0.1	77
26	An integrated view of the methane system in the pockmarks at Vestnesa Ridge, 79°N. Marine Geology, 2017, 390, 282-300.	2.1	74
27	Structure, temporal evolution, and heat flux estimates from the Lucky Strike deepâ€sea hydrothermal field derived from seafloor image mosaics. Geochemistry, Geophysics, Geosystems, 2012, 13, .	2.5	71
28	Temporal variability and tidal modulation of hydrothermal exitâ€fluid temperatures at the Lucky Strike deepâ€sea vent field, Midâ€Atlantic Ridge. Journal of Geophysical Research: Solid Earth, 2014, 119, 2543-2566.	3.4	69
29	Tectonic structure, lithology, and hydrothermal signature of the Rainbow massif (Mid-Atlantic Ridge) Tj ETQq1 1).784314 2.5	rgBT /Overlo
30	Ridge offsets, normal faulting, and gravity anomalies of slow spreading ridges. Journal of Geophysical Research, 1995, 100, 6163-6177.	3.3	66
31	Sensitivity of seafloor bathymetry to climate-driven fluctuations in mid-ocean ridge magma supply. Science, 2015, 350, 310-313.	12.6	65
32	Oceanic corrugated surfaces and the strength of the axial lithosphere at slow spreading ridges. Earth and Planetary Science Letters, 2009, 288, 174-183.	4.4	59
33	Magmatism, serpentinization and life: Insights through drilling the Atlantis Massif (IODP Expedition) Tj ETQq1 1 0	.784314 r 1.4	gBT /Overlo
34	Globally aligned photomosaic of the Lucky Strike hydrothermal vent field (Midâ€Atlantic Ridge,) Tj ETQq0 0 0 rgB Geophysics, Geosystems, 2008, 9, .	T /Overloc 2.5	k 10 Tf 50 1 56
35	The Rheology of the Lower Oceanic Crust: Implications for Lithospheric Deformation at Mid-Ocean Ridges. Geophysical Monograph Series, 0, , 291-303.	0.1	56
36	Fault structure and detailed evolution of a slow spreading ridge segment: the Mid-Atlantic Ridge at 29ŰN. Earth and Planetary Science Letters, 1998, 154, 167-183.	4.4	55

#	Article	IF	CITATIONS
37	Interplay between faults and lava flows in construction of the upper oceanic crust: The East Pacific Rise crest 9°25′-9°58′N. Geochemistry, Geophysics, Geosystems, 2007, 8, n/a-n/a.	2.5	54
38	Extremely asymmetric magmatic accretion of oceanic crust at the ends of slow-spreading ridge segments. Geology, 2000, 28, 179.	4.4	49
39	Tectonic versus magmatic extension in the presence of core complexes at slow-spreading ridges from a visualization of faulted seafloor topography. Geology, 2010, 38, 615-618.	4.4	49
40	A Novel Blending Technique for Underwater Gigamosaicing. IEEE Journal of Oceanic Engineering, 2012, 37, 626-644.	3.8	49
41	Flow Structure and Dispersion within Algal Mats. Estuarine, Coastal and Shelf Science, 1995, 40, 451-472.	2.1	48
42	Quantifying diffuse and discrete venting at the Tour Eiffel vent site, Lucky Strike hydrothermal field. Geochemistry, Geophysics, Geosystems, 2012, 13, .	2.5	47
43	A record of eruption and intrusion at a fast spreading ridge axis: Axial summit trough of the East Pacific Rise at 9–10°N. Geochemistry, Geophysics, Geosystems, 2009, 10, .	2.5	44
44	Magnetic signatures of serpentinization at ophiolite complexes. Geochemistry, Geophysics, Geosystems, 2016, 17, 2969-2986.	2.5	44
45	Quantitative constraint on footwall rotations at the 15°45′N oceanic core complex, Midâ€Atlantic Ridge: Implications for oceanic detachment fault processes. Geochemistry, Geophysics, Geosystems, 2011, 12, .	2.5	43
46	Mapping the Moon: Using a lightweight AUV to survey the site of the 17th century ship â€~La Lune'. , 2013, ,		42
47	Deformation mechanisms of antigorite serpentinite at subduction zone conditions determined from experimentally and naturally deformed rocks. Earth and Planetary Science Letters, 2015, 411, 229-240.	4.4	39
48	Deformation associated with the denudation of mantleâ€derived rocks at the Midâ€Atlantic Ridge 13°–15°N: The role of magmatic injections and hydrothermal alteration. Geochemistry, Geophysics, Geosystems, 2012, 13, .	2.5	38
49	Alteration Heterogeneities in Peridotites Exhumed on the Southern Wall of the Atlantis Massif (IODP) Tj ETQq1 1	0,784314 2.8	4 rgBT /Overl
50	Hydrothermal activity along the slow-spreading Lucky Strike ridge segment (Mid-Atlantic Ridge): Distribution, heatflux, and geological controls. Earth and Planetary Science Letters, 2015, 431, 173-185.	4.4	32
51	Frictional Heating Processes and Energy Budget During Laboratory Earthquakes. Geophysical Research Letters, 2018, 45, 12,274.	4.0	31
52	80-Myr history of buoyancy and volcanic fluxes along the trails of the Walvis and St. Helena hotspots (South Atlantic). Earth and Planetary Science Letters, 2007, 261, 432-442.	4.4	30
53	Regional seismicity of the Mid-Atlantic Ridge: observations from autonomous hydrophone arrays. Geophysical Journal International, 2010, 183, 1559-1578.	2.4	30
54	Magmatic plumbing at Lucky Strike volcano based on olivineâ€hosted melt inclusion compositions. Geochemistry, Geophysics, Geosystems, 2015, 16, 126-147.	2.5	30

#	Article	IF	CITATIONS
55	Dependence of seismic coupling on normal fault style along the <scp>N</scp> orthern <scp>M</scp> idâ€ <scp>A</scp> tlantic <scp>R</scp> idge. Geochemistry, Geophysics, Geosystems, 2016, 17, 4128-4152.	2.5	30
56	Detachment faults at mid-ocean ridges garner interest. Eos, 1998, 79, 127-127.	0.1	29
57	Atypically depleted upper mantle component revealed by Hf isotopes at Lucky Strike segment. Chemical Geology, 2013, 341, 128-139.	3.3	29
58	Ore component mobility, transport and mineralization at mid-oceanic ridges: A stable isotopes (Zn, Cu) Tj ETQq0 2018, 503, 170-180.	0 0 rgBT / 4.4	Overlock 10 29
59	Genesis of corrugated fault surfaces by strain localization recorded at oceanic detachments. Earth and Planetary Science Letters, 2018, 498, 116-128.	4.4	29
60	Focused volcanism and growth of a slow spreading segment (Mid-Atlantic Ridge, 35°N). Earth and Planetary Science Letters, 2001, 185, 211-224.	4.4	28
61	Hydrothermal circulation at slow-spreading mid-ocean ridges: The role of along-axis variations in axial lithospheric thickness. Geology, 2008, 36, 759.	4.4	28
62	Magmatic and tectonic extension at the Chile Ridge: Evidence for mantle controls on ridge segmentation. Geochemistry, Geophysics, Geosystems, 2016, 17, 2354-2373.	2.5	28
63	Co-seismic and post-seismic deformation, field observations and fault model of the 30 October 2020 Mw = 7.0 Samos earthquake, Aegean Sea. Acta Geophysica, 2021, 69, 999-1024.	2.0	28
64	Upper crustal velocity structure beneath the central Lucky Strike Segment from seismic refraction measurements. Geochemistry, Geophysics, Geosystems, 2010, 11, .	2.5	27
65	Hydrothermal seismicity beneath the summit of Lucky Strike volcano, Mid-Atlantic Ridge. Earth and Planetary Science Letters, 2013, 373, 118-128.	4.4	27
66	Tectonic evolution of 200 km of <scp>M</scp> idâ€ <scp>A</scp> tlantic <scp>R</scp> idge over 10 million years: Interplay of volcanism and faulting. Geochemistry, Geophysics, Geosystems, 2015, 16, 2303-2321.	2.5	26
67	Hydrothermally-induced melt lens cooling and segmentation along the axis of fast- and intermediate-spreading centers. Geophysical Research Letters, 2011, 38, n/a-n/a.	4.0	25
68	Seafloor expression of oceanic detachment faulting reflects gradients in mid-ocean ridge magma supply. Earth and Planetary Science Letters, 2019, 516, 176-189.	4.4	25
69	Jet Instability over Smooth, Corrugated, and Realistic Bathymetry. Journal of Physical Oceanography, 2019, 49, 585-605.	1.7	24
70	Automatic scale estimation of structure from motion based 3D models using laser scalers in underwater scenarios. ISPRS Journal of Photogrammetry and Remote Sensing, 2020, 159, 13-25.	11.1	24
71	Fault responsible for Samos earthquake identified. Temblor, 0, , .	0.0	24
72	Parallel bands of seismicity at the Mid-Atlantic Ridge, 12-14°N. Geophysical Research Letters, 2003, 30, .	4.0	23

#	Article	IF	CITATIONS
73	Threeâ€dimensional geometry of axial magma chamber roof and faults at Lucky Strike volcano on the Midâ€Atlantic Ridge. Journal of Geophysical Research: Solid Earth, 2015, 120, 5379-5400.	3.4	23
74	Hydration due to high-T brittle failure within in situ oceanic crust, 30°N Mid-Atlantic Ridge. Earth and Planetary Science Letters, 2008, 275, 348-354.	4.4	22
75	Lucky Strike seamount: Implications for the emplacement and rifting of segmentâ€centered volcanoes at slow spreading midâ€ocean ridges. Geochemistry, Geophysics, Geosystems, 2014, 15, 4157-4179.	2.5	22
76	Crustal accretion at a sedimented spreading center in the Andaman Sea. Geology, 2016, 44, 351-354.	4.4	22
77	Active Long-Lived Faults Emerging Along Slow-Spreading Mid-Ocean Ridges. Oceanography, 2012, 25, 94-99.	1.0	21
78	First direct observation of coseismic slip and seafloor rupture along a submarine normal fault and implications for fault slip history. Earth and Planetary Science Letters, 2016, 450, 96-107.	4.4	21
79	Pervasive silicification and hanging wall overplating along the 13°20′N oceanic detachment fault (<scp>M</scp> idâ€ <scp>A</scp> tlantic <scp>R</scp> idge). Geochemistry, Geophysics, Geosystems, 2017, 18, 2028-2053.	2.5	21
80	Seismological constraints on the thermal structure along the Lucky Strike segment (Mid-Atlantic) Tj ETQq0 0 0 G Geophysical Researches, 2009, 30, 105-120.	rgBT /Over 1.2	rlock 10 Tf 50 20
81	Rare gas systematics on Lucky Strike basalts (37°N, North Atlantic): Evidence for efficient homogenization in a long-lived magma chamber system?. Geophysical Research Letters, 2011, 38, n/a-n/a.	4.0	18
82	The Rheology and Morphology of Oceanic Lithosphere and Mid-Ocean Ridges. Geophysical Monograph Series, 0, , 63-93.	0.1	18
83	The Kallisti Limnes, carbon dioxide-accumulating subsea pools. Scientific Reports, 2015, 5, 12152.	3.3	18
84	Mechanical decoupling and thermal structure at the East Pacific Rise axis 9°N: Constraints from axial magma chamber geometry and seafloor structures. Earth and Planetary Science Letters, 2008, 272, 19-28.	4.4	16
85	Seismic Signatures of Hydrothermal Pathways Along the East Pacific Rise Between 9°16′ and 9°56′N. Journal of Geophysical Research: Solid Earth, 2017, 122, 10,241.	3.4	16
86	Expedition 357 summary. Proceedings of the International Ocean Discovery Program, 0, , .	0.0	16
87	Sedimentation on young ocean floor at the Mid-Atlantic Ridge, 29 °N. Marine Geology, 1998, 148, 1-8.	2.1	15
88	Heat flow variations on a slowly accreting ridge: Constraints on the hydrothermal and conductive cooling for the Lucky Strike segment (Mid-Atlantic Ridge, 37°N). Geochemistry, Geophysics, Geosystems, 2006, 7, n/a-n/a.	2.5	15
89	Alongâ€axis hydrothermal flow at the axis of slow spreading Midâ€Ocean Ridges: Insights from numerical models of the Lucky Strike vent field (MAR). Geochemistry, Geophysics, Geosystems, 2014, 15, 2918-2931.	2.5	15
90	Seismic and magnetic anisotropy of serpentinized ophiolite: Implications for oceanic spreading rate dependent anisotropy. Earth and Planetary Science Letters, 2007, 261, 590-601.	4.4	14

#	Article	IF	CITATIONS
91	Permeability of the Lucky Strike deep-sea hydrothermal system: Constraints from the poroelastic response to ocean tidal loading. Earth and Planetary Science Letters, 2014, 408, 146-154.	4.4	13
92	Controls on the seafloor exposure of detachment fault surfaces. Earth and Planetary Science Letters, 2019, 506, 381-387.	4.4	13
93	Fault Stability Across the Seismogenic Zone. Journal of Geophysical Research: Solid Earth, 2020, 125, e2020JB019670.	3.4	13
94	IODP Expedition 304 & 305 Characterize the Lithology, Structure, and Alteration of an Oceanic Core Complex. Scientific Drilling, 2006, , .	0.6	13
95	A noninvasive method for measuring the velocity of diffuse hydrothermal flow by tracking moving refractive index anomalies. Geochemistry, Geophysics, Geosystems, 2010, 11, .	2.5	12
96	Scale Accuracy Evaluation of Image-Based 3D Reconstruction Strategies Using Laser Photogrammetry. Remote Sensing, 2019, 11, 2093.	4.0	12
97	Automated classification and thematic mapping of bacterial mats in the North Sea. , 2013, , .		11
98	Origin of oceanic ferrodiorites by injection of nelsonitic melts in gabbros at the Vema Lithospheric Section, Mid Atlantic Ridge. Lithos, 2020, 368-369, 105589.	1.4	11
99	Expedition 357 methods. Proceedings of the International Ocean Discovery Program, 0, , .	0.0	11
100	Response to Comment on "Sensitivity of seafloor bathymetry to climate-driven fluctuations in mid-ocean ridge magma supplyâ€: Science, 2016, 352, 1405-1405.	12.6	9
101	Investigating Fineâ€Scale Permeability Structure and Its Control on Hydrothermal Activity Along a Fastâ€Spreading Ridge (the East Pacific Rise, 9°43′–53′N) Using Seismic Velocity, Poroelastic Response, Numerical Modeling. Geophysical Research Letters, 2019, 46, 11799-11810.	and	9
102	Geochemistry of serpentinized and multiphase altered Atlantis Massif peridotites (IODP Expedition) Tj ETQq0 0 0 1 594, 120681.	rgBT /Ovei 3.3	rlock 10 Tf 5 9
103	A short electromagnetic profile across the Kane Oceanic Core Complex. Geophysical Research Letters, 2010, 37, .	4.0	6
104	Machine Tools Anomaly Detection Through Nearly Real-Time Data Analysis. Journal of Manufacturing and Materials Processing, 2019, 3, 97.	2.2	6
105	Rifting Processes at a Continentâ€Ocean Transition Rift Revealed by Fault Analysis: Example of Dabbahuâ€Mandaâ€Hararo Rift (Ethiopia). Tectonics, 2019, 38, 190-214.	2.8	6
106	Shallow-water hydrothermalism at Milos (Greece): Nature, distribution, heat fluxes and impact on ecosystems. Marine Geology, 2021, 438, 106521.	2.1	6
107	SANTORY: SANTORini's Seafloor Volcanic ObservatorY. Frontiers in Marine Science, 2022, 9, .	2.5	6
108	Toxic spill caught Spain off guard. Nature, 1998, 395, 110-110.	27.8	5

#	Article	IF	CITATIONS
109	Monitoring and Observatories: Multidisciplinary, Time-Series Observations at Mid-Ocean Ridges. Oceanography, 2007, 20, 128-137.	1.0	5
110	Oceanographic Signatures and Pressure Monitoring of Seafloor Vertical Deformation in Near-coastal, Shallow Water Areas: A Case Study from Santorini Caldera. Marine Geodesy, 2016, 39, 401-421.	2.0	5
111	Simulation of the 2004 tsunami of Les Saintes in Guadeloupe (Lesser Antilles) using new source constraints. Natural Hazards, 2020, 103, 2103-2129.	3.4	5
112	Terrestrial shallow water hydrothermal outflow characterized from out of space. Marine Geology, 2020, 422, 106119.	2.1	5
113	Fluid Circulation Along an Oceanic Detachment Fault: Insights From Fluid Inclusions in Silicified Brecciated Fault Rocks (Midâ€Atlantic Ridge at 13°20′N). Geochemistry, Geophysics, Geosystems, 2021, 22, .	2.5	5
114	Deep oceanic submarine fieldwork with undergraduate students: an immersive experience with the Minerve software. Solid Earth, 2021, 12, 2789-2802.	2.8	5
115	Tectonic termination of oceanic detachment faults, with constraints on tectonic uplift and mass wasting related erosion rates. Earth and Planetary Science Letters, 2022, 584, 117449.	4.4	5
116	Integrating Multidisciplinary Observations in Vent Environments (IMOVE): Decadal Progress in Deep-Sea Observatories at Hydrothermal Vents. Frontiers in Marine Science, 2022, 9, .	2.5	5
117	Performing submarine field survey without scuba gear using GIS-like mapping in a Virtual Reality environment. , 2019, , .		4
118	Quantification of Gravitational Mass Wasting and Controls on Submarine Scarp Morphology Along the Roseau Fault, Lesser Antilles. Journal of Geophysical Research F: Earth Surface, 2021, 126, e2020JF005892.	2.8	4
119	Age and Rate of Accumulation of Metalâ€Rich Hydrothermal Deposits on the Seafloor: The Lucky Strike Vent Field, Midâ€Atlantic Ridge. Journal of Geophysical Research: Solid Earth, 2022, 127, .	3.4	4
120	Challenges of close-range underwater optical mapping. , 2011, , .		3
121	Optical methods to monitor temporal changes at the seafloor: The Lucky Strike deep-sea hydrothermal vent field (Mid-Atlantic Ridge). , 2013, , .		3
122	Response to Comment on "Sensitivity of seafloor bathymetry to climate-driven fluctuations in mid-ocean ridge magma supply― Science, 2016, 353, 229-229.	12.6	3
123	Simulation of the 2004 tsunami of Les Saintes in Guadeloupe (Lesser Antilles). , 2019, , .		3
124	Radioactivity Monitoring in Ocean Ecosystems (RAMONES). , 2021, , .		3
125	New insights into the plumbing system of Santorini using helium and carbon isotopes. Geochemical Perspectives Letters, 0, , 46-50.	5.0	3
126	Effects of Substrate Composition and Subsurface Fluid Pathways on the Geochemistry of Seafloor Hydrothermal Deposits at the Lucky Strike Vent Field, Midâ€Atlantic Ridge. Geochemistry, Geophysics, Geosystems, 2022, 23, .	2.5	3

#	Article	IF	CITATIONS
127	K-Ar Geochronology and geochemistry of underwater lava samples from the Subsaintes cruise offshore Les Saintes (Guadeloupe): Insights for the Lesser Antilles arc magmatism. Marine Geology, 2022, 450, 106862.	2.1	3
128	Spanish recruitment openly favours insiders. Nature, 1999, 401, 112-112.	27.8	2
129	Differing Views on Science in Spain. Science, 2003, 300, 51c-52.	12.6	2
130	Direct geologic evidence for oceanic detachment faulting: The Mid-Atlantic Ridge, 15°45′N: Comment and Reply. Geology, 2003, 31, e15-e15.	4.4	2
131	Mid-Ocean Ridges and Their Geomorphological Features. , 2021, , .		2
132	Extrusive upper crust formation at slow-spreading ridges: Fault steering of lava flows. Earth and Planetary Science Letters, 2021, 576, 117202.	4.4	2
133	Direct geologic evidence for oceanic detachment faulting: The Mid-Atlantic Ridge, 15°45′N: Comment and Reply. Geology, 2003, 31, e14-e14.	4.4	1
134	Extremely asymmetric magmatic accretion of oceanic crust at the ends of slow-spreading ridge segments. Geology, 2000, 28, 179-182.	4.4	1
135	Modes of seafloor generation at a melt-poor ultraslow-spreading ridge. Geology, 2006, 34, 605.	4.4	1
136	IODP Expeditions 304 and 305 - Oceanic Core Complex Formation, Atlantis Massif. Scientific Drilling, 2005, , .	0.6	1
137	Automated quantification of gradient defined features. , 2008, , .		0
138	Chemical Mass Balance, Depositional Efficiency, and Rates of Formation of Seafloor Massive Sulfide Deposits. , 2020, , .		0